# Airborne gamma-ray spectrometer mapping for relating indoor radon concentrations to geological parameters in the Fen region, southeast Norway

**Björn Henning Heincke[1], Mark A. Smethurst[1], Arne Bjørlykke[1], Sven Dahlgren[2], Jan Steinar Rønning[1,3] and John Olav Mogaard[1]**

*[1] Geological Survey of Norway (NGU), 7491 Trondheim, Norway.*
*[2]Geological advisor, Buskerud, Telemark and Vestfold, Fylkeshuset, 3126 Tønsberg, Norway.*
*[3]Norwegian University of Science and Technology (NTNU), 7491Trondheim, Norway.*
*E-mail: bjorn.heincke@ngu.no*

Extremely high thorium and considerable uranium concentrations are observed in carbonatite rocks of the Fen Complex—an alkaline intrusive complex in southern Norway. Since uranium-bearing bedrock and its weathering products are responsible for increased radon-222 concentrations in nearby dwellings, knowledge about the uranium concentrations of the individual rock types is important for evaluating the associated health risk. Earlier core-sample and ground-based scintillator measurements were limited in relating geological setting to indoor concentrations of radon-222 in such a region with very small-scale geological variations. We have performed airborne radiometric measurements over the entire Fen Complex and the nearby town of Ulefoss. The processed airborne data show that regions dominated by different carbonatite types vary significantly in mean thorium concentrations, but have similar uranium concentrations. Despite the complexity of the region, the obtained thorium/uranium ratios have proven to be a well-suited measure to distinguish regions that are dominated by specific carbonatite types. Furthermore, derived ground-concentration maps enable us to compare uranium ground concentrations directly with indoor radon concentrations of 139 individual dwellings in the Fen region. A positive correlation between local uranium concentrations and percentage of dwellings with indoor radon concentrations > 200 Bq $m^{-3}$ was observed in regions where bedrock or its weathering material crops out. Similarly, high radon concentrations were observed for all carbonatites, indicating that the associated health hazard is largely independent of the dominant carbonatite type. In regions covered by clayey marine sediments, gamma radiation from bedrock is strongly attenuated. Also, indoor radon concentrations are predominantly low because radon transport is strongly limited by the low permeability of the marine sediments.

Heincke, B.H., Smethurst, M.A., Bjørlykke, A., Dahlgren, S., Rønning, J.S. and Mogaard, J.O. (2008) Airborne gamma-ray spectrometer mapping for relating indoor radon concentrations to geological parameters in the Fen region, southeast Norway. *In* Slagstad, T. (ed.) *Geology for Society*, Geological Survey of Norway Special Publication, **11**, pp. 131–143.

## Introduction

The Fen Complex, an intrusive complex of alkaline rocks and carbonatites (carbonate rocks of magmatic origin), is located in Nome municipality, Telemark county, southeast Norway (Figure 1). The eastern parts of the complex are extremely rich in rare earth elements and the radioactive element thorium-232, and to a much lesser degree uranium-238 (Landreth 1979). Concentrations of thorium in this eastern part of the complex are so significant that Norway is considered to host one of the world's largest thorium deposits (OECD NEA and IAEA 2006).


*Figure 1. Map of the Fen region in the Telemark county (southern Norway). Locations of former mining-related activities are highlighted.*

Health hazards associated with the daughter products of uranium and to a lesser extent thorium are of substantial interest for the residents in the Fen region (Sundal and Strand 2004). In particular, inhalation of radon-222 gas, a daughter of uranium, is considered as health risk. After smoking, long-term inhalation of radon is regarded as the second leading cause of lung cancer worldwide (e.g., ICRP 1981, Conrath and Kolb 1995, Strand et al. 2001, Argonne National Laboratory 2005) and is estimated to be responsible for about 280 cases of lung cancer in Norway each year (Smethurst et al. 2006). In a study from Sundal and Strand (2004), the average indoor radon level in the Fen region was determined to be 204 Bq $m^{-3}$ and 37% of the investigated dwellings had radon levels above the intervention level of 200 Bq $m^{-3}$ (see the Norwegian Radiation Protection Agency website at http://www.nrpa.no). This radon level is significantly above the average level in Norway of 88 Bq $m^{-3}$ (Strand et al. 2001). Therefore, it is important to characterise in what way radon concentrations in dwellings vary with bedrock type and type of superficial deposits. With this knowledge, buildings with potential for elevated indoor radon concentrations and suitable, new residential areas can be located more easily.

Health hazards associated with the thorium daughter radon-220 are often neglected within buildings. Radon-220 is short-lived (half-life of 55.6 s) and predominately decays before migrating into houses. In the Fen Complex, most dwellings—excluding houses containing building materials (slags) from the ancient Fen iron mines, which were located within the most thorium-enriched zones—show no increased radon-220 level (Stranden 1984, Stranden and Strand 1986). However, because thorium is far more abundant than uranium in the Fen region, outdoor dose rates (Stranden and Strand 1986) and in mines (Stranden 1985) are mostly dominated by thorium products, and the health hazard presented by radon-220 may potentially be hazardous in future mining activities (Solli et al. 1985).

The Fen Complex became famous in the geological community in 1921, after Brøgger published his classic work (Brøgger 1921). He discovered that carbonates in the Fen Complex were of magmatic origin, and became one of the first proponents of the existence of carbonate magmas. He introduced the term 'carbonatite' for carbonate rocks of apparent magmatic origin, and named rock types in this suite after localities in the Fen region. Since then, the Fen Complex has been investigated by many researchers due to its specific geology and resource potential. Sæther (1957), Barth and Ramberg (1966) and Heinrich (1966) described the general geology. Landreth (1979) summarised the results of an early joint-venture exploration programme evaluating the mineral potential of the region. Exposure-rate measurements in the Fen iron mines (Figure 1) in the 1950s showed that the Fen Complex included rocks with high thorium concentrations (Svinndal 1973). Svinndal (1973) determined thorium concentrations in samples taken along roads, paths and from boreholes and mine galleries in the late 1960s and early 1970s. Dahlgren (1983) published a map showing gamma-ray exposure rates 1 m above the ground over the Fen Complex around the nearby town of Ulefoss. Comparison with measurements on core samples showed that extremely high thorium concentrations, accompanied by elevated uranium concentrations in the carbonatites, were responsible for the high exposure rates. Between 1993 and 2000, indoor radon measurements were carried out in about 250 dwellings in Nome municipality by the company Labnett and the Norwegian Radiation Protection Authority. Sundal and Strand (2004) made a quantitative comparison between 95 of the indoor radon measurements, indoor dose-rate measurements and thorium, uranium and potassium concentrations in 38 rock samples from the nearby bedrock. On this basis, they discussed the influence of bedrock types and superficial deposits on indoor radon concentrations. A similar study based on indoor and outdoor dose-rate measurements in and around 22 dwellings, and investigation of 23 rock samples was published by Stranden and Strand (1986). Stranden (1985) made various radiometric investigations within and nearby the abandoned mines.

These earlier studies give an overview of the geological factors that influence health hazards associated with radon in the Fen region (Dahlgren 1983, Stranden 1984, Stranden and Strand 1986, Sundal and Strand 2004); however, uranium

and thorium concentrations obtained from rock-sample analyses are spot readings that may not reflect the average nuclide concentrations in geologically complex areas like the Fen region. This can lead to a reduced correlation between indoor radon concentrations and uranium concentrations in samples taken from the underlying bedrock. Ground-based scintillator measurements detected such local-scale variations in gamma-ray exposure rates (Dahlgren 1983). However, not all parts of the Fen Complex could be systematically surveyed using ground-level measurements due to high topographic relief, vegetation and limited accessibility of premises. In addition, gamma-ray exposure-rate measurements provide no information on the identities of the radionuclides present in the ground.

To account for these limitations, the Geological Survey of Norway carried out a helicopter-based gamma-ray spectrometer survey in October 2006 to map explicitly near-surface thorium, uranium and potassium concentrations in the Fen region. Because gamma-ray spectrometer measurements determine concentrations by integrating over finite surface areas, average near-surface concentrations of natural radionuclides are possibly better described by airborne spectrometry than by ground-based measurements. Furthermore, maps from detailed airborne surveying provide what is essentially 2D radionuclide coverage of a region and can be related to spatially varying geological phenomena like overburden and bedrock geology. In doing so, airborne surveying can further refine our understanding of the effects of geology on indoor radon concentrations (Smethurst et al. 2006, 2008, submitted).

Already, several other studies in Norway (Walker 1994, Smethurst et al. 2006, 2008, submitted), Canada (Doyle et al. 1990, Ford et al. 2000), Sweden (Åkerblom 1995) and the U.S. (Nielson et al. 1991) have demonstrated that uranium ground concentrations determined from airborne surveys provide a qualitative first-order approximation of regional variation in indoor radon levels under favourable geological conditions (e.g., regions where bedrock is exposed (Åkerblom 1995)). These studies emphasise that airborne data are only suited for identifying areas with an elevated likelihood of encountering high radon concentrations in dwellings. They cannot be used to identify individual dwellings with elevated radon concentrations because several other factors affect the actual indoor radon concentrations, like emanation coefficient, soil permeability, soil diffusivity, pressure conditions, wind, indoor–outdoor temperature differences, house construction and ventilation (e.g., Nazaroff 1992).

## Geology

The Fen Complex has an irregular, oval-shaped surface structure of about 2.3 x 3.0 km (Figure 2a), and formed when alkaline magmas intruded Precambrian gneisses in the Late Neoproterozoic. The complex is dated by $^{40}Ar/^{39}Ar$, giving an average age of 583 ± 15 Ma (Meert et al. 1998). Like other carbonatite areas in Scandinavia (Eckermann 1948, Paarma 1970, Puustinen 1971), the Fen Complex is related to crustal thinning during the break-up of Baltica from Laurentia (e.g., Meert et al. 1998, 2007). Today, only the feeder pipe is visible at the surface because the upper 1–2 km of the former volcanic edifice has been eroded away. Gravity modelling shows that the Fen Complex extends to at least 15 km depth (Ramberg 1973).

The principal types of carbonatite in the Fen Complex are søvite (a calcite carbonatite), rauhaugite (ankeritic or ferrodolomitic carbonatite) and rødberg (a hematite-carbonate rock). Steeply dipping iron-ore veins occur mainly in the hematite-rich rødberg (Svinndal 1973, Andersen 1984). Thorium concentrations are particularly high within the rødberg and ankerite carbonatite (rauhaugite) and associated iron-ore veins (Svinndal l973, Dahlgren 1983).

An outer halo of fenite (100–400 m wide) surrounds most of the Fen Complex, but is best preserved along the western and southern margins. The fenites formed through alkali metasomatism of country gneisses in the contact zones with certain carbonatitic and alkali-silicate magmas. In this process, $SiO_2$ was replaced by $Na_2O$, $K_2O$ and other constituents. In the Fen region, the fenite rocks grade into unaltered granitic gneisses with increasing distance from the carbonatite complex.

Basic alkaline silicate rocks of the ijolite and melteigite group (rocks consisting of nepheline and pyrorxene) occur in the southwestern part of the complex. A minor area in the south-central part of the complex consists of vipetoite; a coarse-grained cumulate rock consisting of amphibole, pyroxene, phlogopite and apatite. Damtjernite, a porphyritic ultramafic lamprophyre with megacrysts of phlogopite, amphibole, pyroxene and olivine, occurs as minor bodies scattered within the Fen Complex (Bergstøl and Svinndal 1960, Dahlgren 1994).

Diatremes and dykes of damtjernite, and dykes of carbonatite and phonolite ('tinguaites') penetrate the Proterozoic basement surrounding the Fen Complex, and have been discovered up to 47 km from the complex (Dahlgren 1987, 1994).

The country rock in the Fen region is predominantely composed of medium-grained gneissic granite with interlayered units of mica schists, amphibolite and mica-rich gneisses.

The Fen region was located below sea level after the last glacial period and has risen about 140 m in the past 10,000 years (Bergstrøm 1984). Therefore, large parts of the Fen Complex are covered by post-glacial allochthonous marine silt and clay deposits (~60% of the surface area, Figure 2b) that can reach a thickness of several tens of metres (Bergstrøm 1984). In the Fen region, the bedrock or its weathering products only locally crop out at the surface. In the southern part of the region, the bedrock is partly covered by glacial moraine deposits (Figure 2b).

The Fen Complex has a rather interesting mining history. The Fen iron mines were operated between AD 1657 and 1927 in the eastern part of the Fen Complex, i.e., within the areas

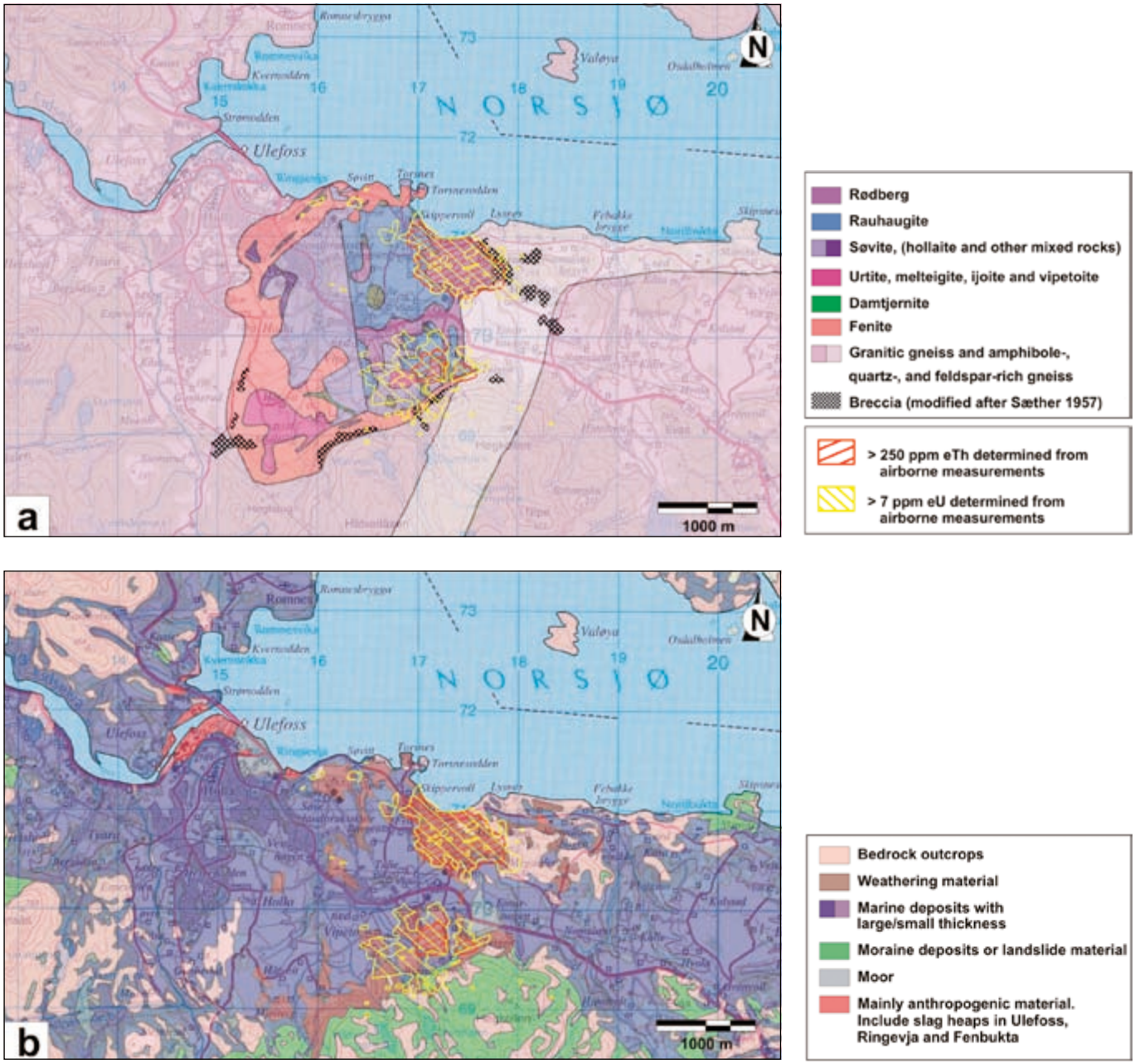


*Figure 2. (a) Geological and (b) Quaternary map from the Fen region (modified after NGU database). Red and yellow lines highlight areas with high thorium (> 250 ppm eTh) and significant uranium concentrations (> 7 ppm eU) at the surface, respectively. The concentrations were derived from the airborne gamma-ray spectrometer data.*

consisting of the high-Th rødberg rocks. Niobium and iron was exploited both in open pits and underground mines in the northwestern part of the complex, i.e., within the low-Th søvitic rocks (Bjørlykke and Svinndal 1960, Dahlgren 2005) (Figure 1). Over the centuries, material from the ancient Fen iron mines was carried to the Ulefoss Iron Works, and cast-bricks made from slag during the iron ore melting were extensively used in the area for house construction (e.g., Ulefoss farm, Holden farm and Holla church, Dahlgren 1983, Stranden and Strand 1986, Dahlgren 2005).

## Measurements and processing of radiometric data

Helicopter measurements were carried out using a 256-channel Exploranium GR820 gamma-ray spectrometer with sodium iodide detector packs with a total crystal volume of 20.9 l (16.7 l downward and 4.2 l upward directed). An area of about 20 $km^2$ over the Fen Complex and nearby town of Ulefoss was surveyed. To ensure a uniform and dense data coverage, the measurements were performed along parallel lines with a narrow line spacing of 50 m. The average flying altitude during the measurements was 45 m and an average speed of 70 km $h^{-1}$ resulted in measurement intervals of about 20 m. Referring to a formula given by Grasty (1987), we expect that about 80% of the gamma-ray counts for a single measurement come from an area on the ground with radius 90 m assuming a height of 45 m and no movements. With a line spacing of 50 m we can assume measurement overlap between adjacent flight lines and deduce that the airborne survey provides 2D data coverage of the region.

Processing of the airborne gamma-ray spectrometer data began with noise reduction of full-spectrum data using the NASVD method (Minty and Hovgaard 2002). Spectral windows were then live-time corrected and aircraft and cosmic background values removed (e.g., IAEA 2003). The spectral-ratio method of Minty (1998) was used to remove the effects of radon in the air below and around the helicopter. Window stripping was used to isolate count rates from the individual radionuclides K, U and Th (IAEA 2003). The topography in parts of the Fen region is rough (15–290 m above sea level), and stripped window count rates were corrected both for variations in ground clearance and ground geometry (Schwarz et al. 1992). Residual line-level errors—remaining inconsistencies between adjacent flight lines—were removed by passing a median filter over the data set (Mauring and Kihle 2006). Finally, radionuclide count rates were converted to ground element concentrations using calibration values derived from calibration pads at the Geological Survey of Norway in Trondheim. The processed data are shown in three maps: equivalent thorium concentration (eTh) in ppm in Figure 3a, equivalent uranium concentration (eU) in ppm in Figure 3b, and potassium concentration in % in Figure 3c.

## Results and interpretation

Thorium and uranium concentrations vary strongly in the surveyed region (Figures 3a, b), reflecting the complex geology of the region (Figures 2a, b) and human activities like mining and ore smelting (generating spoil and slag heaps). Only a few decimetres of fine-grained marine sediments are enough to effectively shield gamma radiation emitted by underlying thorium- and uranium-bearing rocks. Consistent with this, areas of fine-grained marine deposits in the Fen area (Figure 2b) are marked by low concentrations of thorium (< 20 ppm eTh, Figure 3a) and uranium (< 4 ppm eU, Figure 3b) on our maps.

Where rocks of the volcanic complex and their weathering products are at or near the land surface, we observe extremely high thorium concentrations (up to 1460 ppm eTh at Gruveåsen) and significant uranium concentrations (up to 27.3 ppm eU around Rullekollhaugen) (Figures 3a, b). Thorium-232 levels of other typical Nordic rock types are much lower, with a range of 0.5–350 Bq $kg^{-1}$, corresponding to ~ 0.12–88 ppm Th (Nordic 2000). Radium-226 levels above 150 Bq $kg^{-1}$, corresponding to ~ 12.2 ppm U, are observed in Norway, not only in carbonatites, but also alum shale and radium-rich granites (Nordic 2000). At first glance, a first-order correlation between thorium and uranium concentrations seems to exist in the carbonatites. However, we will see in the following discussion that the thorium/uranium ratio varies significantly between the different rock types.

In many parts of the surveyed region, human activities significantly affect thorium and uranium ground concentrations derived from the airborne data. In particular, thorium and uranium anomalies on the factory site of the Ulefoss mill (up to 111 ppm eTh and 5.2 ppm eU) are obviously caused by radioactivity from slagheap material (see Figures 1 and 3a, b). The natural uranium and thorium ground concentrations in this area are surely low. Moreover, two uranium anomalies on the premises of the Søve niobium mine area are associated with waste heaps (Dahlgren 2005). Additional excavations and heaps from mining activities and construction can disturb the original ground concentrations and accordingly can affect the estimates for thorium and uranium concentrations of individual rock types derived from airborne data.

Potassium concentrations in the Fen area are in the common range and reach 8.5% (Figure 3c). We want to remark that a distinct transition zone separates areas with larger (> 2.5%) and smaller (< 2%) potassium concentrations in the southeast and in the east of the surveyed region. This radiometric boundary coincides with the transition zone from the feldspar-rich gneissic county rocks and fenites (enriched in potassium by metasomatism) to potassium-poorer carbonatites in the Fen Complex. Analyses of rock samples, presented by Sundal and Strand (2004), also show that fenites have significantly higher potassium concentrations (~ 3.4%) than all kinds of carbonatites (< 1.5%).

Results of our airborne data are consistent with the ones of earlier ground-based exposure-rate measurements (Dahlgren 1983). (Dahlgren (1983) presented terrestrial gamma radiation in exposure rate (µR $h^{-1}$). However, today terrestrial gamma radiation is expressed in dose rate absorbed in air (nGy $h^{-1}$). To be consistent with the publication from Dahlgren (1983), we decided to use exposure rate µR h-1 in this contribution. Conversion to SI-units is: 1 µR $h^{-1}$ = 8.69 nGy $h^{-1}$ (IAEA 2003).) Although only the most inhabited areas were densely surveyed by Dahlgren (1983), the extrapolated extent of areas with exposure rates > 20 µR $h^{-1}$ resembles areas revealed by airborne surveying to have > 40 ppm Th and > 4 ppm U (Figures 3a, b). Moreover, areas with very high exposure rates of 100 µR

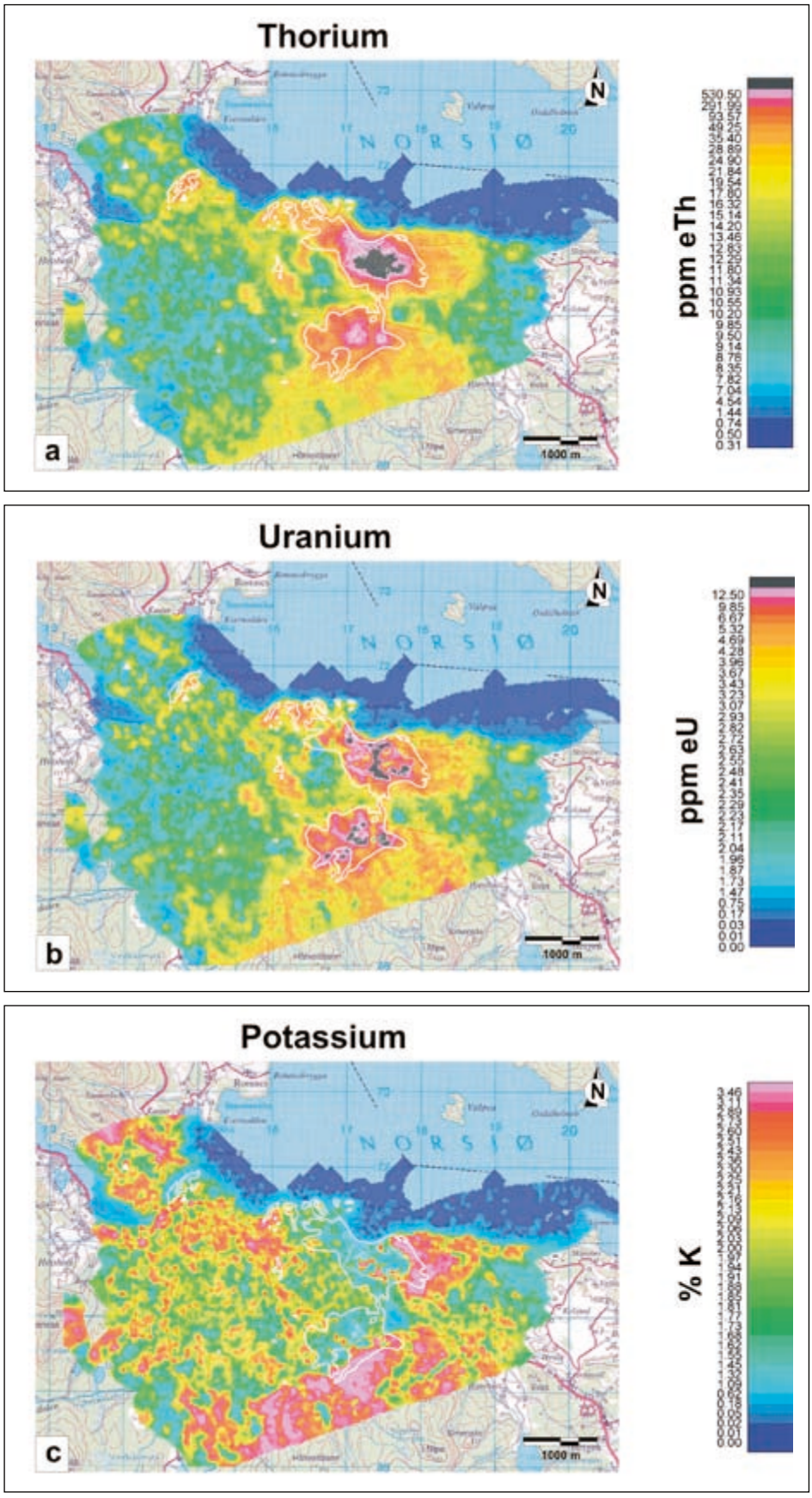


*Figure 3. Ground concentrations of the natural radioactive elements (a) thorium, (b) uranium and (c) potassium, obtained from airborne gamma-ray spectrometer measurements are shown in three colour plots. Black colours in (a) and (b) indicate areas with more than 560 ppm eTh and 13 ppm eU, respectively. Continuous and dashed lines encompass areas with exposure rates of more than 20 and 100 μR $h^{-1}$ derived from ground-based scintillator measurements in the early 1980s (Dahlgren 1983). White triangles mark the locations of the farmyards Holden and Ulefoss. They are built up from blocks that were cast of slag from the Ulefoss Iron Works.*

$h^{-1}$ generally coincide with areas having thorium concentrations greater than 290 ppm. Concentrations of 4 ppm U, 40 ppm Th and 290 ppm Th are theoretically equivalent to exposure rates of 2.6, 11.48 and 83.23 μR $h^{-1}$, respectively, assuming radioactive equilibrium in the decay series (IAEA 1989). Considering an average potassium concentration of about 1.5% (see Figure 3c), corresponding to 2.26 μR $h^{-1}$, absolute values from the exposure-rate and airborne measurements are comparable.

## Comparing results from airborne measurements and rock-sample analyses to quantify Th and U concentrations for different carbonatite types

Results from our airborne measurements and previous rock-sample analyses showed that high thorium concentrations are predominantly found within ankerite and hematite carbonatite rocks in the Fen region (see Table 1). Results from airborne measurements indicate highest thorium concentrations in the region around Gruveåsen, consisting mainly of rødberg carbonatites (183–1460 ppm eTh, Figure 3a). Significantly lower, but still very high thorium concentrations are observed in rødberg carbonatites around Rullekollhaugen and in rauhaugite carbonatites at various localities (33.4–586 and 17.7–545 ppm eTh, respectively). Lower, but still significant concentrations are observed in regions dominated by søvite carbonatites (10.3–150 ppm eTh, see Table 1 and Figure 4). In contrast to thorium concentrations, uranium concentrations derived from airborne measurements are relatively similar for the three carbonatite rock types. Mean values of 10.7, 9.1 and 7.1 ppm eU were obtained for rødberg, rauhaugite and søvite, respectively (see Table 1, Figures 3b and 4).

Results from various rock-sample analyses (Svinndal 1973, Dahlgren 1983, Stranden and Strand 1986, Sundal and Strand 2004) (Table 1) show the same order of decreasing thorium concentrations from rødberg through rauhaugite to søvite carbonatites in the Fen Complex. Except for søvite, mean thorium concentrations from different rock-sample analyses are in the same range (see Table 1). Thorium concentrations measured from rock samples are also in the same range as the concentrations determined from airborne investigations with the exception of rødberg around Gruveåsen. For Gruveaåsen, rock-sample analyses by Dahlgren (1983) gave values of 560–3000 ppm Th, whereas the airborne investigation yielded 229–620 ppm eTh. Svinndal (1973) found that increasing concentrations of thorium from søvite to rødberg is very closely linked to the increasing hematite content. He reported highest thorium concentrations in core samples from a hematite-ore heap of the Fen iron mine (up to 4200 ppm) and from a 2 m-thick hematite vein within the rødberg carbonatites (2400–3100 ppm).

Uranium concentrations from different rock-sample investigations vary strongly between the carbonatite types. For example, søvite samples described by Stranden and Strand (1986) have a factor 15 (!) higher mean uranium concentrations than the ones from Sundal and Strand (2004) (Table 1). Referring to Sundal and Strand (2004), søvite is the carbonatite type with the lowest mean uranium concentrations, but Stranden and Strand (1986) present søvite as the carbonatite type with the highest mean uranium concentrations. In a similar way, rock-sample results from Stranden and Strand (1986) show that rødberg carbonatites have higher uranium concentrations than rauhaugite carbonatites, but results from Sundal and Strand

*Table 1. Thorium- and uranium-concentrations for different rock types. Results from rock samples are taken from Dahlgren (1983), Stranden and Strand (1986) and Sundal and Strand (2004). For the airborne data, only regions where the bedrock or its weathering material is visible at the surface are considered to derive the thorium and uranium concentrations. Mean values are written in parentheses.*

| | Core samples | | | | | | | | | | Airborne investigations | | |
|---|---|---|---|---|---|---|---|---|---|---|---|---|---|
| | Thorium (ppm) | | | | | Uranium (ppm) | | | | | eTh | eU | n |
| Rock type | *I* | *II*[1] | n | *III*[1] | n | *I* | *II*[1] | n | *III*[1] | n | | | |
| Granitic gneiss | 2.5–31.0 | – | 0 | 15.7–17 (16.5) | 3 | 1.3–9.0 | – | 0 | 3.5–3.7 (3.6) | 3 | 5.3–141.0 (28)[2] | 0.8–13.3 (3.8)[2] | 356 |
| Fenite | ~ 10 | 45.6 | 1 | 5–50 (32.5) | 8 | ~ 2.5 | 0.6 | 1 | 3.3–6.5 (4.1) | 8 | 8.2–44.2 (20) | 1.7–7.8 (3.9) | 148 |
| Søvite | 1–50 | 2.5–192 (76) | 6 | 5–48 (20) | 9 | 1–60 | 0.8–113 (25) | 6 | 0.8–4.9 (1.6) | 9 | 10.3–150 (56) | 1.9–17.5 (7.1) | 103 |
| Rauhaugite | <2000 | 39–1724 (138) | 4 | 72.5–232 (150) | 9 | – | 1.6–23.4 (10.5) | 4 | 3.3–24.4 (9.8) | 9 | 17.7–545 (232) | 2.1–22.6 (9.1) | 137 |
| Rødberg (Gruveåsen) | 560–3000 | 41–2950 (985) | 12 | 97–1475 (775) | 9 | 5–40 | 3.5–44.5 (12.9) | 12 | 1.6–8.9 (5.7) | 9 | 183–1460 (620) | 1.8–25.1 (10.7) | 259 |
| Rødberg (Rullekoll-haugen) | 160–330 | | | | | 3.5–20 | | | | | 33.4–586 (229) | 4.0–27.3 (10.8) | 25 |

[1] Stranden and Strand (1986) and Sundal and Strand (2004) presented activity concentrations in Bq $kg^{-1}$. Activity concentrations are converted to corresponding thorium, uranium and potassium concentrations (IAEA 2003).

[2] Gneiss on the Gruveåsen, in the vicinity of rødberg, are not considered here.

References: *I*: Dahlgren (1983); *II*: Stranden and Strand (1986); *III*: Sundal and Strand (2004).

n = number of samples. The number of samples from Dahlgren (1983) is unknown.

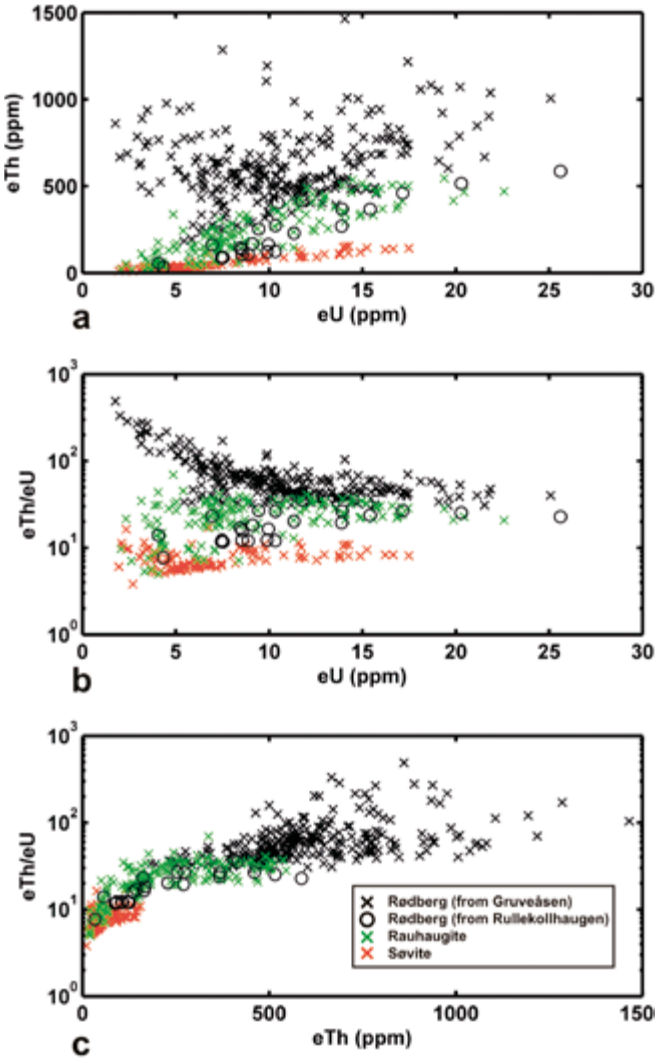


*Figure 4. Relationships between (a) uranium and thorium concentrations, (b) thorium/uranium ratio and uranium concentration, and (c) thorium/uranium ratio and thorium concentration for different rock types. Each data point is related to the thorium and uranium ground concentrations from an individual airborne spectrometer measurement after processing. Only points in regions where bedrock or its weathering material is mapped at the surface are considered. Regions dominated by the carbonatites søvite and rauhaugite are marked with red and green crosses, respectively. Rødberg carbonatites from the Gruveåsen and close to the Rullekollhaugen are shown as black crosses and black circles, respectively.*

(2004) show the opposite. Particularly in rock-sample analyses from Dahlgren (1983) and Stranden and Strand (1986), the obtained uranium concentrations vary a lot for individual carbonatite types.

These inconsistencies indicate the limitations of rock-sample investigations to provide 'average' uranium (and thorium) concentrations in the geologically very complex Fen region. It is difficult to classify carbonatites by uranium content and accordingly to assess their associated radon risk from analysis of individual samples. In contrast, concentrations obtained from airborne spectrometry represent an average property of the rocks within an area on the ground of some hundreds of square meters and thus lend themselves to establishing large-scale geochemical differences between rock types with complex internal variations.

## Thorium/uranium ratios

Although søvite, rauhaugite and rødberg have similar uranium concentrations (Figure 4), the ratio of thorium-to-uranium concentration is a very suitable parameter to distinguish the three carbonatite types. Except for rødberg-dominated rocks around Rullekollhaugen (thorium/uranium ratios of 10–30), rødberg-dominated rocks have clearly higher thorium/uranium ratios (> 25 around the Gruveåsen) than rauhaugite-dominated rocks (~ 10–30 west of Gruveåsen and around Rullekollhaugen). Areas dominated by søvite have significantly lower ratios (< 10), like in the central western part of the volcanic region and in Vipeto, southwest of Rullekollhaugen. Around Rullekollhaugen, the boundary between rauhaugite- and søvite-dominated areas coincides with a border that separates regions with higher (> 14) and lower (< 12) thorium/uranium ratios (see Figures 2a and 5). This is a remarkable correlation considering the limited spatial resolution of airborne investigations, the geological complexity of this area and the strong variation in uranium concentrations observed in the rock samples for each carbonatite type.

Different thorium/uranium ratios for the carbonatite types are in agreement with the outdoor gamma count rates measured by Stranden and Strand (1986). They noted that in rødberg-, rauhaugite- and søvite-dominated areas, 97%, 85% and 58%, respectively, of the total count rates originated from thorium. Similar uranium levels, but strongly varying thorium levels in søvite, rauhaugite and rødberg also explain Sundal and Strand's (2004) observation that there is only a weak correlation between indoor gamma dose rates and indoor radon concentrations in the Fen Complex. It is also consistent with geochemical mapping of stream sediments from Ryghaug (1986) that gave no indication of a correlation between thorium and uranium concentrations in the Fen Complex.

Our results are also in agreement with investigations from carbonatite complexes all over the world. Wolley and Kempe (1989) suggested average thorium/uranium ratios of 6, 7 and nearly 40 for calcio-, magnesio- and ferrocarbonatites, respectively, based on investigations of various carbonatite complexes. Our ratios of 7.9, 25.5 and 54.7 for søvite (a calcite carbonatite), rauhaugite (ankeritic or ferrodolomitic carbonatite) and rødberg (a hematite carbonate rock), respectively, are in agreement with but slightly higher than the general ratios, possibly indicating weathering effects responsible for depletion of uranium relative to thorium. Andersen (1984) suggested that rødberg and the associated hematite-ore veins formed by secondary hydrothermal oxidation processes from the pre-existing rauhaugite. How such secondary processes can change actual uranium and thorium concentrations was not mentioned in this publication.

Most regions consisting of fenites and gneissic country rocks are characterised by low thorium/uranium ratios (< 12). However, east of the rødberg-dominated part of Gruveåsen, high thorium/uranium ratios are observed in gneiss as far as 250 m away from the carbonatite area. This compositional boundary is not a sharp one, but related to 'rødberg' veining

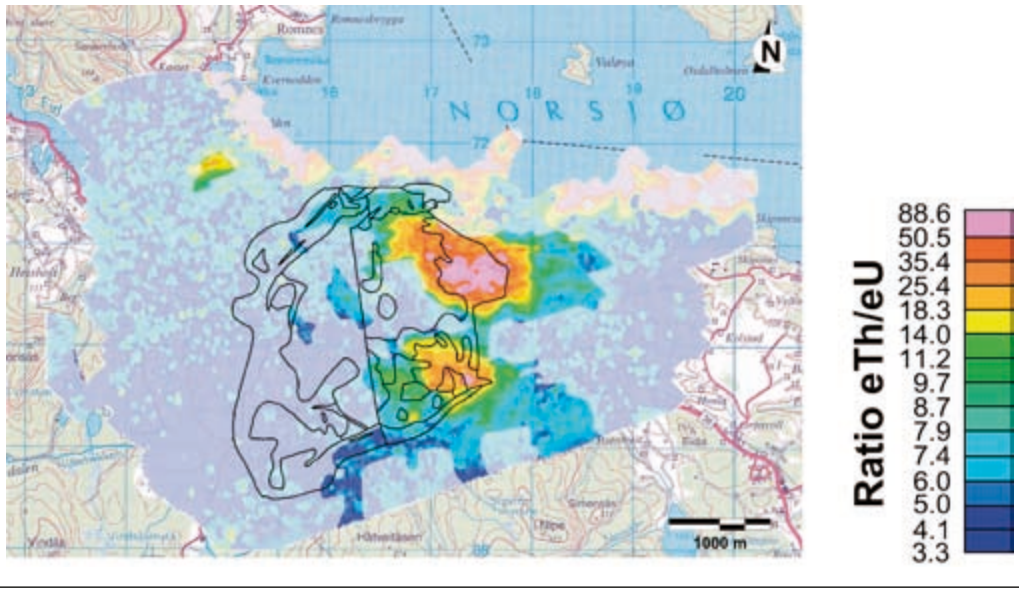


*Figure 5. Ratios of thorium and uranium concentrations determined from airborne gamma-ray spectrometer data. To focus on regions whose ratios are not affected by sediment coverage, regions with low thorium and/or uranium concentration (threshold: ppm eTh + 15 x ppm eU < 70) are covered with a semi-transparent mask. Boundaries of geological units (see Figure 2a) are indicated with black lines.*

and carbonatite as matrix in brecciated gneiss (see Figure 2a) associated with ubiquitous secondary alteration (Andersen 1984). Areas dominated by damtjernite, vipeotite, urtite, iljoite and melteigite rocks are relatively small (Ramberg 1973) and their radionuclide concentrations are difficult to estimate from the airborne data. However, determination of low uranium and thorium ground concentrations in the southwestern part of the complex (see Figures 2a, b) suggest that iljoite-melteigite rocks are not enriched in natural radionuclides.

## Relating uranium concentrations to indoor radon concentrations

Dense airborne surveying and accurate drift geology and bedrock geology maps enable a detailed analysis of the relationship between geology and indoor radon concentrations. For this purpose, we considered indoor radon concentrations measured by the Norwegian Radiation Protection Authority in 139 dwellings in Nome municipality (Figure 6). The indoor measurements were carried out with CR–39 etched track detectors (Sundal and Strand 2004). Since the radon diffusion half-time of the detector design is greater than a few minutes, measurements are considered to be insensitive to radon-220. The majority of indoor radon-concentration measurements were performed from February until May 2000 and the data were corrected for seasonal variations. One hundred and six of the indoor radon measurements were collected in 2000, and 33 were collected in the winter of 1996/97. Although two measurements were conducted in each dwelling (usually in the living room and in the


*Figure 6. Indoor radon concentration in the Fen region. Coloured circles indicate locations of houses, for which results from indoor radon-concentration measurements are available. Red colours mark regions where either the bedrock or its weathering products crop out at the surface (see also Figure 2b). Yellow line sketches the extent of the volcanic region (see also Figure 2a). Results from indoor radon-concentration measurements based on material provided by Nome municipality.*

bedroom nearest the ground), we consider here only the highest value. Because Nome municipality and its residents are generally aware that radon is associated with specific rock types in the Fen Complex, the majority of measurements are in dwellings standing on carbonatites (Figure 6). Thorium-/uranium-rich material from the Fen region was not used in the considered dwellings, and Sundal and Strand (2004) reported that building materials used for houses in the Fen region contain low levels of radioactivity. We had, unfortunately, no adequate data about the dwellings such that influence from building construction and ventilation could not be investigated. Radon from water supplies is not considered a dominant indoor radon source in the Fen region (Dahlgren 1983, Ryghaug 1984, Stranden 1985).

Average indoor radon concentrations in houses built on marine deposits are distinctly lower (mean value: 160 Bq $m^{-3}$; 22% above 200 Bq $m^{-3}$) than in houses built directly on bedrock or its weathering products (mean value: 350 Bq $m^{-3}$; 69% above 200 Bq $m^{-3}$) (Figures 6 and 7a). The marine sediments are mainly silts with significant clay contents of 19–20% (Bergstrøm 1984). Although fine-grained sediments may have a high radon emanation coefficient (e.g., Greeman and Rose 1996), their low permeability prohibits transport of the radon produced in them towards dwellings. Also, because clayey material is virtually impermeable, only a small portion, if any, of the radon gas emanating from bedrock beneath the clay layer is likely to reach the dwellings (Åkerblom 1986, Nazaroff 1992). This is unless a construction punctures the marine layer, exposing the structure to radon from deeper sources.

Although distinctly lower than on bedrock, the incidence of elevated radon levels in dwellings on the marine deposits is still high in the Fen region. These elevated radon levels could be caused by local variations in the nature of the substrate (e.g., higher portion of coarse-grained material) not evident in the generalised drift geology map, and/or the possible presence of radium-bearing soil in places. It is also possible that some spots in the clayey marine deposits with higher radium concentrations remain invisible to airborne spectrometry because clays' high moisture content leads to an increased attenuation of the radioactivity in the soil, thus underestimating the actual radioactive-element ground concentrations (Wilford et al. 1997). Finally, Åkerblom (1986), who described indoor radon risks in Sweden, emphasised that for all soil conditions there is a risk that indoor radon levels will exceed 200 Bq $m^{-3}$ if sufficient quantities of soil gas leak into the house due to bad sealing.

In areas where the bedrock or its weathered products are exposed, radon concentrations in indoor air vary strongly (10–1292 Bq $m^{-3}$; $\sigma$ = 271.7 Bq $m^{-3}$) and the percentage of dwellings with indoor radon concentrations above 200 Bq $m^{-3}$ is 69%.

Only a very weak positive correlation is observed between indoor radon concentrations and uranium ground concentrations determined from the airborne data (see Figure 7a), consistent with observations from other studies (e.g., Smethurst et al. submitted). Locally, radon concentrations vary widely because indoor radon measurements are strongly influenced by the positions of the rooms that are measured, home construction methods, heating and ventilation solutions,

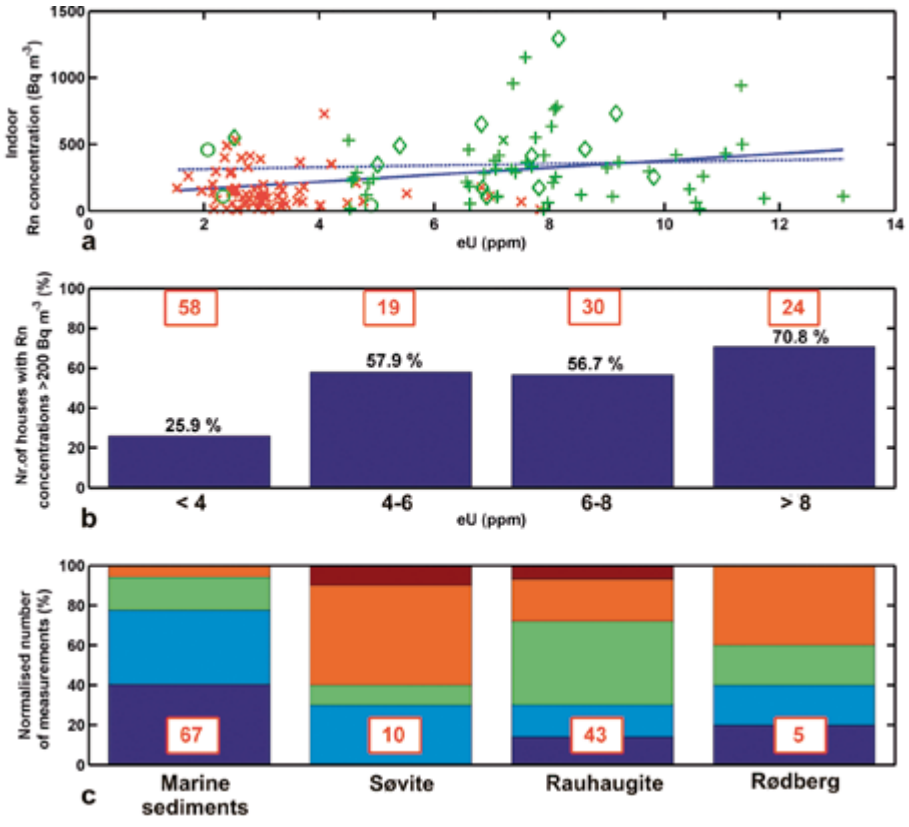


*Figure 7. (a) Relationship between uranium ground concentrations and radon indoor activity concentrations. Uranium ground concentrations are derived from the processed airborne gamma-ray spectrometer data at the locations of houses in which the radon concentration was measured. The red and green colours indicate houses built on ground consisting of unconsolidated marine sediments and outcropping rock/weathering material, respectively. For constructions placed on rock/weathering material, the dominant rock types are distinguished by different symbols: rauhaugite/rødberg (+), søvite (◊), fenite (x) and gneisses (o). The blue, continuous line describes the best linear fit to all data. It has an axis intercept of 113 Bq $m^{-3}$, a slope of 26.4 Bq $m^{-3}$ ppm and a linear correlation coefficient of 0.316. The blue, dashed line describes the best linear fit to data from houses built on rock/weathering material. It has an axis intercept of 300 Bq $m^{-3}$, a slope of 6.7 Bq $m^{-3}$ ppm and a linear correlation coefficient of 0.47. (b) Histogram showing the percentages of dwellings with indoor radon concentrations > 200 Bq $m^{-3}$ for different ranges of uranium ground concentrations. (c) Normalised histogram showing the indoor radon concentrations for marine sediments and different rock types cropping out at the surface. In (b) and (c), the corresponding number of measurements are plotted in the red boxes.*

the presence of openings in the structure to the ground, local ground conditions, especially permeability in the ground, and local variation in radon emanation coefficients (e.g., Nazaroff 1992). This invariably complicates attempts to establish relationships between indoor radon concentrations and outdoor measurements made above the ground. Nevertheless, some studies (Ford et al. 2000, Smethurst et al. submitted) demonstrate that there can be a distinct correlation between uranium ground concentrations from airborne investigations and percentages of dwellings with indoor radon concentrations above a specific threshold. This kind of relationship also seems to hold for indoor radon and equivalent uranium measurements for the Fen region. The percentage of dwellings with indoor radon concentrations over 200 Bq $m^{-3}$ are plotted against equivalent uranium concentrations, obtained from airborne measurements, in Figure 7b. The trend is less pronounced than observed in the studies of Ford et al. (2000) and Smethurst et al. (2006, 2008, submitted), presumably due to the lower number of indoor radon measurements available in the Fen region.

There is no clear relationship between indoor radon concentrations and different carbonatite types (see Figures 6 and 7c). This is to be expected because the airborne measurements indicate similar average uranium concentrations for the different carbonatite types. It seems that gneisses outside of the Fen Complex cause lower indoor radon concentrations than all carbonatite types. However, too few indoor measurements are available from the gneissic region to verify this observation.

Like us, Sundal and Strand (2004) observed fewer high radon concentrations in dwellings on marine deposits than on exposed bedrock (carbonatite)[1]. Again, like us, they observed that radon levels are similar in dwellings on different carbonatite types and they suggested that high indoor radon concentrations were caused by søvite, rauhaugite and rødberg rocks in the building ground. They mentioned that uranium concentrations determined from their rock samples (see Table 1) may not be representative for søvite rocks because there is a contradiction of the low uranium concentrations in their rock samples and high indoor levels in the adjacent dwellings.

## Conclusions

Airborne gamma-ray spectrometer measurements provided us with three maps showing ground concentrations of thorium-232, uranium-238 and potassium-40 in the Fen Complex and around the nearby town of Ulefoss. Extremely high thorium concentrations, and significant uranium concentrations, were observed in parts of the Fen Complex that were not covered by post-glacial marine sediments. The highest thorium concentrations are found in the area around the Gruveåsen (up to 1460 ppm eTh). We observe very different thorium concentrations in the different carbonatite lithologies (mean values: 425 ppm eTh (rødberg), 232 ppm eTh (rauhaugite) and 56 ppm eTh (søvite)), but mean uranium concentrations are relatively similar (mean values: 10.7 ppm eU (rødberg), 9.1 ppm eU (rauhaugite) and 7.1 ppm eU (søvite)). Thorium/uranium ratios from our airborne data are suited for differentiating between the different carbonatites and can be used to refine and improve our knowledge of the spatial distribution of these lithologies.

Results from airborne investigations are in agreement with the results from former investigations (rock-sample studies and ground-based scintillator measurements). However, airborne investigations are less sensitive to small-scale variations in radionuclide concentration than rock-sample measurements, and probably better represent average concentrations for individual rock types in the complex Fen region.

Percentages of dwellings with indoor radon concentrations > 200 Bq $m^{-3}$ correlate with increasing uranium ground concentrations in the Fen region. Where fine-grained, low-permeability marine sediments cover bedrock, uranium concentrations in the ground are low and high radon concentrations in indoor air are less common than in dwellings on other kinds of overburden or bedrock. Where bedrock and associated weathering products are exposed, different carbonatite types exhibit similar distributions of indoor radon concentrations. For all carbonatite types, dwellings were found that had very high indoor radon concentrations > 700 Bq $m^{-3}$ . In summary, elevated radon concentrations occur where carbonatites or their weathered products are close to the surface, and are equally associated with all types of carbonatite.

## Acknowledgements

We thank John Peterson from the Argonne National Laboratory for his very helpful comments about the health risks of thorium and its decay products. Bjørn Ivar Rindstad (NGU) supported us with cartographical material. We thank Per Ryghaug and Håvard Gautneb (NGU) for helpful discussions about correlations of uranium and thorium concentrations in the Fen region, and Morten Rask Arnesen from Nome municipality for providing indoor radon measurements. Terje Strand of Oslo University supported us with important information about their radon measurements and the potential health risk related to radon-220 in the Fen region. The airborne gamma-ray survey was co-financed by Nome municipality and NGU. Agemar Siehl and an anonymous reviewer are thanked for comments that helped improve the paper.

[1] Sundal and Strand (2004) published results from 95 dwellings from the Fen region. It is quite likely that they partly used measurements from the same dwellings that we do. Accordingly, their and our data sets cannot be considered independent. Because information about the actual localities of investigated dwellings were not given in their publication, we did not use their data for relating uranium ground concentrations and indoor radon activities.

## References


Andersen, T. (1984) Secondary processes in carbonatites: petrology of 'rødberg' (hematite-calcite-dolomite carbonatite) in the Fen central complex, Telemark (South Norway). *Lithos*, **17**, 227–245.

Argonne National Laboratory (2005) Human Health Fact Sheet. *Natural Decay Series: Radium*.

Barth, T.F.W. and Ramberg, I.B. (1966) The Fen circular complex. *In* Tuttle, O.F. and Gittens, J. (eds.) *Carbonatites*, John Wiley and Sons, New York, pp. 225–257.

Bergstøl, S. and Svinndal, S. (1960) The carbonatities and per-alkaline rocks of the Fen area. *Norges geologiske undersøkelse*, **208**, 99–105.

Bergstrøm, B. (1984) Nordagutu. Beskrivelse til kvartærgeologisk kart. *NGU skrifter*, **57**, 44 pp.

Bjørlykke, H. and Svinndal, S. (1960) Fen Region: Mining and exploration work. *Norges geologiske undersøkelse*, **208**, 105–110.

Brøgger, W.C. (1921) Die Eruptivgesteine des Kristianiagebietes: IV. Das Fensgebiet im Telemark, Norwegen. *Det Norske Videnskaps-Akademi i Oslo, Skrifter. I. Mat.-Naturv. Klasse, 1920*, **9**, 408 pp.

Conrath, S.M. and Kolb, L. (1995) The health risk of radon. *Journal of Environmental Health*, **58**, 24–26.

Dahlgren, S. (1983) Naturlig radioaktivitet i berggrunnen, gammastrålingskart, Fensfeltet, Telemark, scale 1:10,000. *'Prosjekt temakart, Telemark'*.

Dahlgren, S. (1987) *The satellitic intrusions in the Fen Carbonatite – Alkaline rock province, Telemark, Southeastern Norway*. PhD thesis, University of Oslo, 350 pp.

Dahlgren, S. (1994) Late Proterozoic and Carboniferous ultramafic magmatism of carbonatitic affinity in southern Norway. *Lithos*, **31**, 141–154.

Dahlgren, S. (2005) Miljøgeologisk undersøkelse av lavradioaktivt slagg fra ferroniobproduksjonen på Søve 1956–1965. *Regiongeologen for Buskerud, Telemark og Vestfold, Rapport nr.1*, 47 pp.

Doyle, P.J., Grasty, R.L. and Charbonneau, B.W. (1990) Predicting geographic variations in indoor radon using airborne gamma-ray spectrometry. *Current Research, Part A, Geological Survey of Canada*, **90–1A**, 27–32.

Eckermann, H. (1948) The alkaline district of Alnö island. *Sveriges Geologiska Undersöking, Serie Ca*, **36**, 9–36.

Ford, K.L., Savard, M., Dessau, J.-C., Pellerin, E., Charbonneau, B.W. and Shives, R.B.K. (2000) The role of gamma-ray spectrometry in radon risk evaluation; a case history from Oka, Quebec. *Geoscience Canada*, **28**, 59–64.

Greeman, D.J. and Rose, A.W. (1996) Factors controlling the emanation of radon and thoron in soils of the eastern U.S.A. *Chemical Geology*, **129**, 1–14.

Grasty, R.L. (1987) The design, construction and application of gamma-ray spectrometer calibration pads–Thailand. *Geological Survey of Canada, Paper 87–10*, 34 pp.

Heinrich, E.W. (1966) *The geology of carbonatites*, Rand McNally and Co., Chicago, 555 pp.

IAEA (1989) Construction and Use of Calibration Facilities for Radiometric Field Equipment. *Technical Reports Series No. 309*, Vienna, Austria.

IAEA (2003) Guidelines for radioelement mapping using gamma ray spectrometry data. *IAEA–TECDOC–1363*, Vienna, Austria. 173 pp.

ICRP (1981) Limits for Inhalation of Radon Daughters by Workers. *International Commission on Radiological Protection (ICRP) Report No. 32*, 24 pp.

Landreth, J.O. (1979) Mineral potential of the Fen Alkaline Complex. Ulefoss. Norway. *Bergvesenet Rapport BV 1332*, 30 pp.

Mauring, E. and Kihle, O. (2006) Levelling aerogeophysical data using a moving differential median filter. *Geophysics*, **71**, L5–L11.

Meert, J.G., Torsvik, T.H., Eide, E.A. and Dahlgren S. (1998) Tectonic Significance of the Fen Province, S. Norway: Constraints from Geochronology and Paleomagnetism. *The Journal of Geology*, **106**, 553–564.

Meert, J.G., Walderhaug, H.J., Torsvik, T.H. and Hendriks, B.W.H. (2007) Age and paleomagnetic signature of the Alnö carbonatite complex (NE Sweden); additional controversy for the Neoproterozoic paleoposition of Baltica. *Precambrian Research*, **154**, 159–174.

Minty, B.R.S. (1998) Multichannel models for the estimation of radon background in airborne gamma-ray spectrometry. *Geophysics*, **63**, 1986–1996.

Minty, B.R.S. and Hovgaard, J. (2002) Reducing noise in gamma-ray spectrometry using spectral component analysis. *Exploration Geophysics*, **33**, 172–176.

Nazaroff, W.W. (1992) Radon transport from soil to air. *Reviews of Geophysics*, **30**, 137–160.

Nielson, D.L., Cui, P. and Ward, S.H. (1991) Gamma-Ray Spectrometry and Radon Emanometry in Environmental Geophysics. *Investigations in Geophysics*, **5**, 219–250.

Nordic (2000) Naturally occurring radioactivity in the Nordic countries–recommendations. *The Radiation Protection Authorities, Denmark, Finland, Iceland, Norway and Sweden*, 80 pp. See also: http://www.ssi.se/english/Flaggboken.pdf (05.11.2007).

OECD NEA and IAEA (2006) *Uranium 2005: Resources, Production and Demand*, OECD Publishing, 388 pp.

Paarma, H. (1970) A new find of carbonatite in North Finland, the Sokli plug in Savukoski. *Lithos*, **3**, 129–133.

Puustinen, K. (1971) Geology of the Siilinjärvi carbonatite complex, Eastern Finland. *Bulletin de la Commission geologique de Finlande*, **249**, 1–43.

Ramberg, I.B. (1973) Gravity studies of the Fen Complex, Norway, and their petrological significance. *Contributions to Mineralology and Petrology*, **38**, 115–134.

Ryghaug, P. (1984) En uran-anomali i Telemark og dennes innvirkning på radon-innholdet i drikkevann. *Vann*, **2**, 172–181.

Ryghaug, P. (1986) Stream-sediment geochemical survey of the Fen carbonatite/alkaline complex and surrounding areas. *Prospecting in Areas of Glaciated Terrain*, **7**, 187–200.

Schwarz, G.F., Klingele, E.E. and Rybach, L. (1992) How to handle rugged topography in airborne gamma-ray spectrometry surveys. *First Break*, **10**, 11–17.

Smethurst, M.A., Strand, T., Finne, T.E. and Sundal, A.V. (2006) Gammaspektrometriske flymålinger og radon: anvendelse av gammaspektrometriske fly- og helikoptermålinger til identifisering av radonutsatte områder—analyse basert på målinger på Østlandet *StrålevernRapport 2006:12*, 20 pp., Østerås: Statens strålevern.

Smethurst, M.A., Sundal, A.V., Strand, T. and Bingen, B. (2008) Testing the performance of a recent radon-hazard evaluation in the municipality of Gran, eastern Norway. *In* Slagstad, T. (ed.) *Geology for Society*, Geological Survey of Norway Special Publication, **11**, in press.

Smethurst, M.A., Strand, T., Sundal, A.V. and Rudjord, A.L. (submitted) A novel approach to radon-hazard mapping: Utilizing relationships between airborne gamma-ray spectrometer measurements and indoor radon concentrations. *Science of the Total Environment*.

Solli, H.M., Andersen, A., Stranden, E. and Langård, S. (1985) Cancer incidence among workers at a niobium mine. *Scandinavian Journal of Work, Environment & Health*, **11**, 7–13.

Strand, T., Ånestad, K., Ruden, L., Ramberg G.B., Jensen C.L., Wiig, A.H. and Thommesen G. (2001) Kartlegging av radon i 114 kommuner—Kort presentasjon av resultater. *StrålevernRapport 2001:6*, 14 pp., Østerås: Statens strålevern.

Stranden, E. (1984) Thoron ($^{220}$Rn) daughter to radon ($^{222}$Rn) daughter ratios in thorium-rich areas. *Health Physics*, **47**, 784–785.

Stranden, E. (1985) The radiological impact of mining in a Th-rich Norwegian area. *Health Physics*, **48**, 415–420.

Stranden, E. and Strand, T. (1986) Natural gamma radiation in a Norwegian area rich in thorium. *Radiation Protection Dosimetry*, **16**, 325–328.

Sundal, A.V. and Strand, T. (2004) Indoor gamma radiation and radon concentrations in a Norwegian carbonatite area. *Journal of Environmental Radioactivity*, **77**, 175–189.

Svinndal, S. (1973) Thorium i Fensfeltet. *NGU Report 1162*, 28 pp.

Sæther, E. (1957) The alkaline rock province of the Fen area in southern Norway. *Det Kongelige Norske Videnskabers Selskabs Skrifter*, **1**, 1–150.

Walker, P. (1994) Airborne radon hazard mapping–Løten, Hedmark county, Norway. *NGU Report 1993.046*, 50 pp.

Wilford, J.R., Bierwirth, P.N. and Craig, M.A. (1997) Application of airborne gamma-ray spectrometry in soil/regolith mapping and applied geomorphology. *AGSO–Journal of Australian Geology & Geophysics*, **17**, 201–216.

Wolley, A.R. and Kempe, D.R.C. (1989) Carbonatites: Nomenclature, average chemical compositions and element distribution. *In* Bell, K. (ed.) *Carbonatites—Genesis and Evolution*, Unwin Hyman Ltd., London, pp. 1–14.

Åkerblom, G. (1986) Investigations and mapping of radon risk areas. *In* Wolff, F.C. (ed.) *Geology for environmental planning*, Geological Survey of Norway Special Publication, **2**, 96–106.

Åkerblom, G. (1995) The use of airborne radiometric and exploration survey data and techniques in radon risk mapping in Sweden. Application of uranium exploration data and techniques in environmental studies. *IAEA–Tecdoc*, **827**, 159–180.